Fish and Shellfish Immunology 94 (2019) 294–307

Contents lists available at ScienceDirect

Fish and Shellfish Immunology

journal homepage: www.elsevier.com/locate/fsi

Full length article

Comparative transcriptomics and histopathological analysis of crucian carp infection by atypical *Aeromonas salmonicida*

Xiao-dong Ling[a], Wei-tao Dong[a], Yong Zhang[a], Xu Qian[c], Wang-dong Zhang[a], Wan-hong He[a], Xing-xu Zhao[a,*], Ji-xing Liu[b,**]

[a] College of Veterinary Medicine, Gansu Agricultural University, Lanzhou, 730070, China
[b] Product R & D, Lanzhou Weitesen Biological Technology Co. Ltd., Lanzhou, 730030, China
[c] Animal Husbandry and Fishery Technology Promotion Center of Yuzhong, Yuzhong, 730100, China

ARTICLE INFO

Keywords:
Crucian carp
Aeromonas salmonicida
Transcriptomics
Histopathology

ABSTRACT

Aeromonas salmonicida is a ubiquitous fish pathogen known to cause furunculosis. With the emergence of new subtypes and the expansion of the host range, it has threatened the health of a variety of marine and freshwater fish, particularly the non-salmonids, manifesting differently from the classical furunculosis. Although there have been reports of infection by atypical strains on the crucian carp, the pathogenesis and tissue pathology remain unclear. In this study, transcriptomics and histopathology were used to analyze the immune response and lesions of crucian carp infected with *A. salmonicida*. Comparative analysis showed 6579 differentially expressed genes (DEGs) (3428 down-regulated and 3151 up-regulated) were identified on day 5 post-infection (5 dpi). Further annotation and analysis revealed that the DEGs were enriched in enzyme regulator activity, response to oxidative stress, iron ion homeostasis and other functions, and mitogen-activated protein kinase (MAPK), nuclear factor-κB (NF-κB), toll-like receptor (TLR), and nucleotide-binding oligomerization domain (NOD)-like receptor (NLR) etc., and immune-related signaling pathways. Meanwhile, the four C-type lysozyme genes found in all DEGs were significantly up-regulated after infection. In addition, there was severe bleeding on the body of the infected fish. Also, the intestine, liver, spleen, and kidney showed varying degrees of inflammatory damage, especially the goblet cell hyperplasia of intestinal mucosa epithelium and degeneration and necrosis of renal tubular epithelium cells. Additionally, with the increase in pathogen concentration, the cumulative mortality increased, the severity of lesions in the hindgut and head-kidney tissues increased. The relative expression levels of four immune-related genes (TNF-α, IL-1β, IL-11, C-lysozyme) were also significantly upregulated, compared with the control ($P < 0.05$). In conclusion, this study provides a scientific basis for further study on the immune response, pathological diagnosis, and prevention of crucian carp infection caused by atypical *A. salmonicida*.

1. Introduction

Aeromonas salmonicida is the causative agent of furunculosis, a disease which severely affects marine and freshwater fish cultures, causing significant economic losses in fish farming [1]. While it is best known as a pathogen of salmonids, multiple other species can be infected by atypical isolates or different sub-species [2]. Furthermore, atypical *A. salmonicida* has been isolated from human blood, wild animals, and pork [3–6]. Interestingly, varied clinical signs are associated with the infection in different fish species, although skin ulcerations and hemorrhages are recurrent features [1].

Crucian carp (*Carassius auratus*) is widely distributed in waters around China and is the most widely used economic fish in freshwater aquaculture. Due to high-density cultivation and inappropriate management measures, there have been more frequent outbreaks of the crucian carp disease in recent years. At the same time, new pathogens are emerging. In recent years, there have been reports of the infection of crucian carp by atypical *A. salmonicida*. For example, Han J E et al. isolated *A. salmonicida subsp. achromogenes* from crucian carp and performed genome sequencing [7]. Wistbacka S et al. found that *A. salmonicida subsp. salmonicida* infection can increase thiamine activity in crucian carp tissues [8]. Therefore, with the expansion of the host range of *A. salmonicida*, the healthy cultivation of crucian carp has been endangered.

* Corresponding author. College of Veterinary Medicine, Gansu Agricultural University, 1# Ying Men-cun Road, Lanzhou, 730070, China.
** Corresponding author. Product R & D, Lanzhou Weitesen Biological Technology Co. Ltd., 16# Yan Nan Road, Lanzhou, 730030, China.
E-mail addresses: zhaoxx@gsau.edu.cn (X.-x. Zhao), 15348029930@163.com (J.-x. Liu).

https://doi.org/10.1016/j.fsi.2019.09.006
Received 5 June 2019; Received in revised form 11 August 2019; Accepted 2 September 2019
Available online 03 September 2019

Table 1
Primers used for qRT-PCR in this study.

Primer name	Length	Tm	GC	Sequence
Fc-LP5-F	28	55.9	35.7%	GTGAGCATTAAACCTGATCAACATGTAT
Fc-LP5-R	29	53.4	37.9%	ATCTGATACTGTCAGTGTAACTTCATCAC
IL-8L-F	28	57.3	50.0%	GAAGTCATCTCAGCCAGACTACAGCTAC
IL-8L-R	28	59.9	39.3%	CATAAACTTCTGCATGCAAACACAGATG
Toll-R2-F	28	57.2	46.4%	CTGAGAGAGGTGTACAAGAATGGCTTAG
Toll-R2-R	26	57.4	46.2%	GATTCTGTCGAAGTGTTCGTTCTGAG
LEI-L-F	26	58.5	50.0%	CCTAATCCGACTGCTGATCAGCTATCCGA
LEI-L-R	26	58.5	50.0%	CGTAAGTCTTATCCTTCACCCAGCTG
INIAP-L-F	21	56.5	61.9%	GCAGCAAGCTCTGGAGGACAG
INIAP-L-R	22	57.4	59.1%	CCTCACGCTTGTACTGCTGCAG
INF-IP44-F	27	56.4	44.4%	CTTGAGCTGAGCGACTCTAATGTTAAG
INF-IP44-R	22	55.7	54.5%	TGTCTTCTGGATGAGCTCCCTG
NF-κ-BRF-F	26	61.7	50.0%	CATCTGATGGAACTGAAGAGCCCATG
NF-κ-BRF-R	25	59.8	52.0%	CCAAGGCCACATCCTTACTTCTGTG
IL-6L-F	25	62.8	56.0%	CAGAAGTGGCATCTGATGGCCAGAG
IL-6L-R	28	60.5	50.0%	GCTCCAGTTGTCTTTATACCAGGTCAGG
IL-1β- F	23	55.8	47.8 %	GATGGCATACCAATGCGACATAC
IL-1β- R	25	55.3	44.0 %	GATCACATTCTCCAAGAAGAAGCTG
TNF-α- F	26	57.3	46.2%	GATGGATCTTGAGAGTCAGCTTGTTG
TNF-α- R	24	59.8	54.2%	GTCACCTTGTTGAGCGTGAAGCAG
IL-11-F	26	57.5	46.2 %	GCTGTTGGCTCAACTTCATCTGTTAG
IL-11-R	28	58.2	42.9 %	CTTGAACCTATGGTGATCAATCTCTGTG
C-lysozyme- F	24	61.4	58.3 %	GGCAACTATGTGTGCACGGCCTAC
C-lysozyme -R	22	62.9	63.6 %	ACCTGGAGTGCCGTCATCGCAC
β-actin-F	21	54.1	52.4%	TGGACTTTGAGCAGGAGATGG
β-actin-R	21	52.7	47.6%	CTAGGAAGGATGGCTGGAAAA

Lesions in tissue and cell morphological structure can not only clarify the pathological process and pathogenesis of the disease, but they can also be the basis for identifying and diagnosing different diseases. In the past few decades, there have been many reports on the histopathology of *A. salmonicida* infected various fish species. For example, salmonids [9], atlantic halibut [10], common wolfish [11], catfish [12], cod [13,14] etc. These studies found that most fish had different pathological features except for a few infected fish with typical furunculosis symptoms after infection with A. salmonicida [1]. Unfortunately, the histopathological study of the crucian carp infected with A. salmonicida has not been reported so far.

After pathogens invade the body, they damage the cells and tissues of the host, whereas, the immune organs in the host kill, neutralize, and eliminate the pathogens and their toxic products by regulating the expression of immune-related genes. Studies have shown that the kidney of the teleost is not only a hematopoietic organ, but also an important immune organ of the fish [15], functionally similar to the mammalian bone marrow [16]. At the same time, the teleost's head kidney can differentiate and produce large numbers of lymphocytes, macrophages, and granulocytes as well as secretory antibodies [17–19]. These immune-related cells and antibodies play an important role in immune protection and the elimination of bacteria from the blood [20]. In addition, the main symptoms in fish, following *A. salmonicida* infection, occur in muscles and internal organs, especially the kidney tissues [21]. Therefore, the head kidney tissue of crucian carp can be an important organ in the study of the pathogenic mechanism and immune response of *A. salmonicida.*

At present, transcriptomics is widely used to study the expression of genes in tissues under different physiological conditions. It is useful in the study of molecular mechanisms in specific biological processes and diseases [22–24]. Rapid developments in these techniques have not only accelerated investigations into the process of pathogenic infection and defense strategies in fish but have also been used to identify immunity-related genes.

In this study, we analyzed the immune response of crucian carp to *A. salmonicida* at 5 dpi, using transcriptome profiling. Additionally, we studied the lesion characteristics of crucian carp tissue cells before and after infection. We also studied the relationship between the different concentrations of *A. salmonicida* and severity of histological alterations and immune response. This will provide a basis for the study of the regulation of immune response and pathological changes in the tissues of the crucian carp after infection.

2. Materials and methods

2.1. Fish

Full-sib crucian carps were purchased from a farm in Yongdeng, Gansu Province, China. Each fish weighing approximately 220 g were transferred into a 1000-L aerated water tank and cultured at 20–22 °C for seven days. They were fed pelletized feed (Lexiang Biotech Co., Ltd., Qingdao, China) daily at 2–3% of their body weight. One-half of the water was replaced every two days throughout the experiment.

2.2. Isolation and identification of bacteria

The kidney tissue of the diseased crucian carp was coated with TSA solid medium on a clean bench. After incubation at 18 °C for about 48 h, the clones were picked and cultured. The morphology, color, and size of the colonies were observed. Then, a single colony was picked and examined by Gram staining. The physiological and biochemical characteristics of the strain were determined with reference to "Bergey's Manual of Determinative Bacteriology" [25]. Then the DNA was extracted with a bacterial genomic DNA extraction kit (TIANGEN, Beijing, China). Using the extracted DNA as a template, 27F/1492R was used as a primer for PCR amplification, and the gel recovery product was sequenced. The complementary DNA sequence of the 16S rDNA obtained by sequencing was subjected to Blast analysis with the known nucleic acid sequence in the GenBank database. The nucleic acid sequence having high correlation with the sequence was selected, and the phylogenetic tree was constructed using the MEGA (Molecular Evolutionary Genetics Analysis) software.

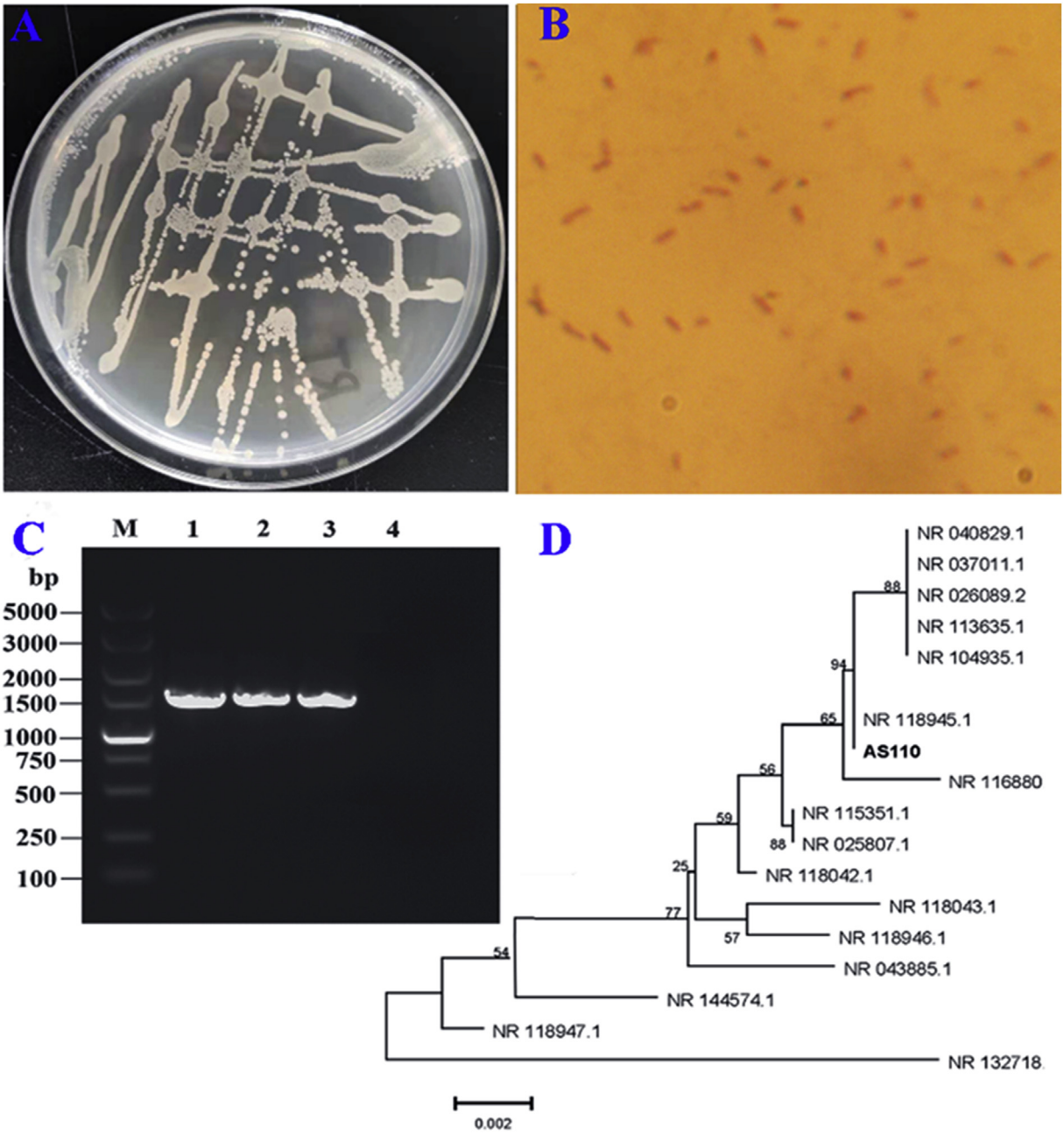

Fig. 1. Isolation and identification of *A. salmonicida*. (A): Monoclonal colonies cultured; B: Gram staining of bacteria; C: PCR-amplified nucleic acid gel using pure culture DNA as template and 27F/1492R as primer; D: Phylogenetic tree based on isolated strain and reference strains.

2.3. Regression infection test and diagnosis of A. salmonicida on crucian carp

All experiments were conducted according to the guiding principles of the Chinese Legislation on the Use and Care of Laboratory Animals. The animal protocol was approved by the Animal Welfare and Research Ethics Committee of Gansu Agricultural University. The anesthesia of crucian carps in this study was 100 ng/ml MS-222.

Eight healthy carps were randomly divided into experimental and control groups, four in each group, and the experimental group was intraperitoneally injected with 0.1 ml concentration 10^7 cfu/mL of live bacteria and control group 0.1 ml of sterile PBS. After 5 days of infection, the kidney tissues from the experimental and the control groups were coated with TSA solid medium and cultured at 18 °C for about 48 h. The bacterial DNA was extracted and used as a template (sterile deionized water was used as the negative control), design primers using the sequence of *A. salmonicida* strain 16S ribosomal RNA gene (accession number: NR_118,945). PCR was performed as follows: 95 °C for 5 min, followed by 32 cycles of 95 °C for 10 s, 58 °C for 30 s, and 72 °C for 60 s. The DNA fragment was sequenced.

2.4. Lethal dose (LD_{50}) of A. salmonicida to crucian carp

The 48 crucian carp (about 220 g) were randomly distributed in six tanks of 100 L (n = 8 fish/tank). Individual colonies were then picked and inoculated into TSA liquid medium, which was incubated at 18 °C and 220 rpm for 48 h. After the bacterial count, serial dilutions were prepared (10^5 to 10^{10} cfu/mL). The fish were inoculated intraperitoneally with 1.5 mL of *A. salmonicida* suspension with different concentrations. The $LD_{50\text{-}7d}$ was estimated using the Spearman-Karber method [26], and the final $LD_{50\text{-}7d}$ for crucian carp was 2.06×10^7 cfu/mL.

Table 2
The biochemical identification of the isolated strain.

Character	A. salmonicida subsp.	Isolates
Growth 37 °C	–	–
Glycerol aerogenesis	+	+
Decompose galactosum	+	+
L - arginine	–	–
L - histidine	–	–
L - glutamic acid	–	–
L - alanine	–	–
7.5% NaCl	–	–
Indole	–	–
Lysine decarboxylase	–	–
V–P test	–	–
H_2S production	–	–
Decompose mannitol	+	+
Decompose arabinose	+	+
Decompose esculin	+	+
Decompose sucrose	–	–
Brown-producing pigment	+	+

Note: "+", positive, "-", negative.

2.5. Crucian carp challenge experiment and sample collection

The 120-tailed crucian carp was randomly divided into control (PBS), low dose infection (10^4 cfu/mL), medium dose infection (10^7 cfu/mL), and high dose infection (10^{10} cfu/mL), each group 30-tailed. Each group was intraperitoneally injected with 0.1 ml of live bacteria at low dose, moderate and high dose, and 0.1 ml of sterile PBS was injected into the control group [27]. The samples were taken at 5 dpi. The crucian carps was first anesthetized in 100 ng/ml MS-222; the abdominal cavity was opened to take samples of the head-kidney and hindgut tissue; it was rinsed with diethylpyrocarbonate-treated water; it was then placed in cryopreservation tube and subsequently stored in liquid nitrogen.

2.6. Histological examination and evaluation of lesion severity

The visceral organs of the fish were sectioned. The intestine, liver, spleen and kidney were fixed with 10% neutral formalin, after one week, they were dehydrated with alcohol, embedded in paraffin, and cut into 4 μm slices, and stained with hematoxylin and eosin and viewed under the light microscope.

We performed histopathological evaluation of the hindgut and head-kidney tissues of the crucian carp infected with high, medium, and low doses of bacteria. The specific evaluation criteria were as follows:

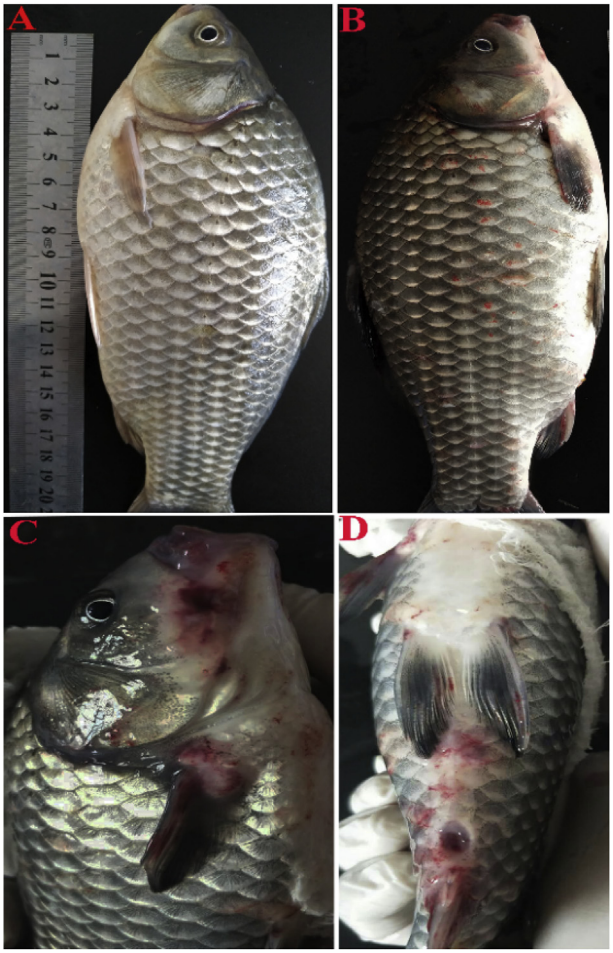

Fig. 3. The crucian carp body surface bleeding symptoms of *A. salmonicida* infection. A: control group; B, C, D are the bleeding of different parts after infection.

(1) According to the integrity of the organizational structure, they were divided into good (0 points), medium injury (1 point), and severe injury (2 points); (2) according to the degree of infiltration of inflammatory cells, they were divided into low (1 point), medium (2 points), and high (3 points); (3) according to the degree of degeneration and necrosis of cells, they were divided into low (1 point), medium (2 points), and high

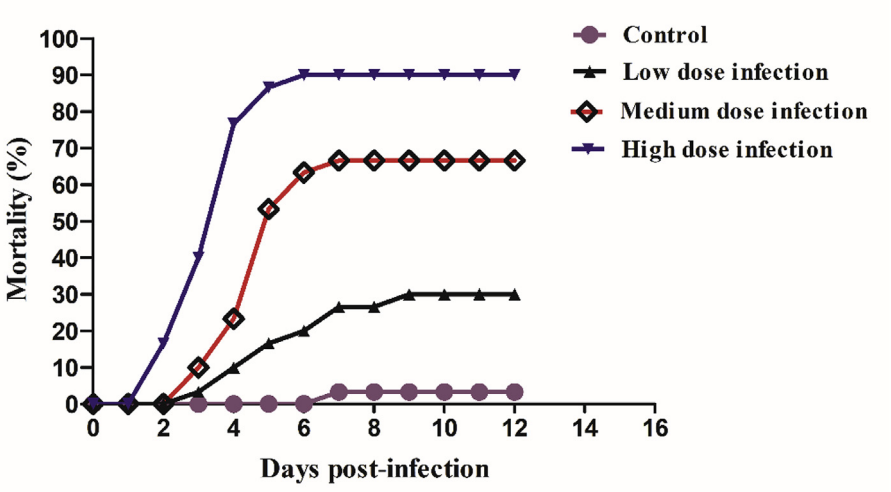

Fig. 2. Cumulative mortality of fish infected with different concentrations of *A. salmonicida*. PBS was the negative control.

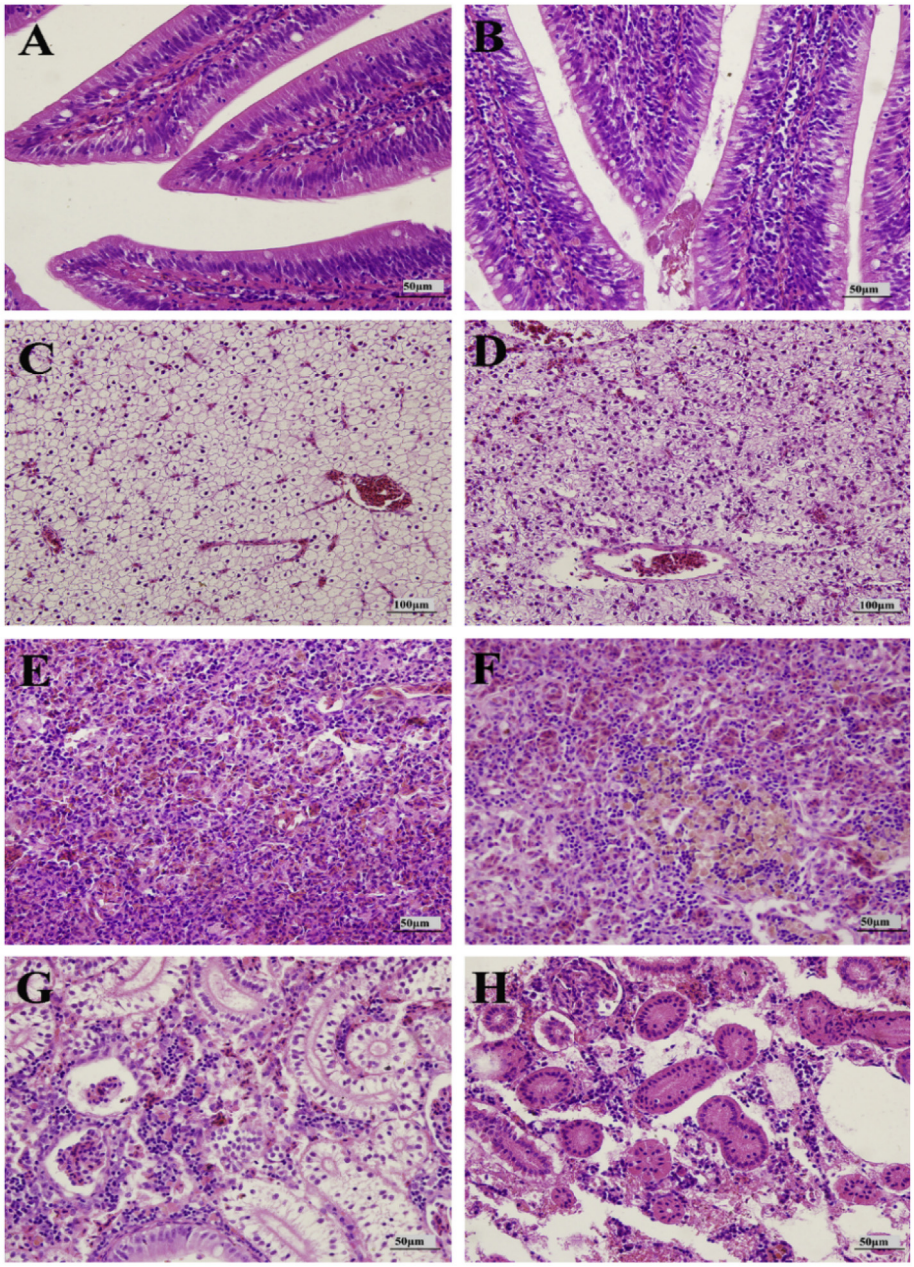

Fig. 4. Hematoxylin-eosin staining of the inner organs of crucian carp infected with *A. salmonicida*. (A) non-infected intestine; (B) infected intestine; (C) non-infected liver; (D) infected liver; (E) non-infected speen; (F) infected speen; (G) non-infected kidney; (H) infected kidney.

(3 points). Finally, the statistical score level determines the severity of the lesion. The higher the score, the more serious the lesion. Statistical analysis (Mann-Whitney test) was conducted using GraphPad Prism software.

2.7. RNA isolation and library preparation

Extraction of total RNA from the head kidney of control and medium concentration infected crucian carp, using standard protocols (Trizol; Invitrogen, USA). mRNA selection, library preparation, and sequencing were performed by the TruseqTM RNA sample prep Kit (Illumina, USA) on an Illumina Hiseq sequencer, according to manufacturer's specifications. Briefly, mRNA was purified from total RNA using poly-T oligo-attached magnetic beads. Fragmentation was carried out using divalent cations under elevated temperature in NEB Next First Strand Synthesis Reaction Buffer. First strand cDNA was synthesized using random hexamer primer and M-MuLVReverse Transcriptase. Second strand cDNA synthesis was subsequently performed using DNA Polymerase I and RNase H. After adenylation of 3′ ends of DNA fragments, NEB Next Adaptor with hairpin loop structure were ligated to prepare for hybridization. In order to select cDNA fragments of preferentially 250–300 bp in length, the library fragments were purified with AMPure XP system (Beckman Coulter, Beverly, USA). Then PCR was performed with Phusion High-Fidelity DNA polymerase, Universal PCR primers and Index (X) Primer. Lastly, PCR products were purified (AMPure XP system) and library quality was assessed on the Agilent Bioanalyzer 2100 system.

2.8. Illumina sequencing, assembly, and differential gene expression analysis

Raw reads (FastQ) were processed through in-house scripts: clean data were obtained by removing reads containing adapter, reads containing ploy-N and low quality reads from raw data. Then the Q20,

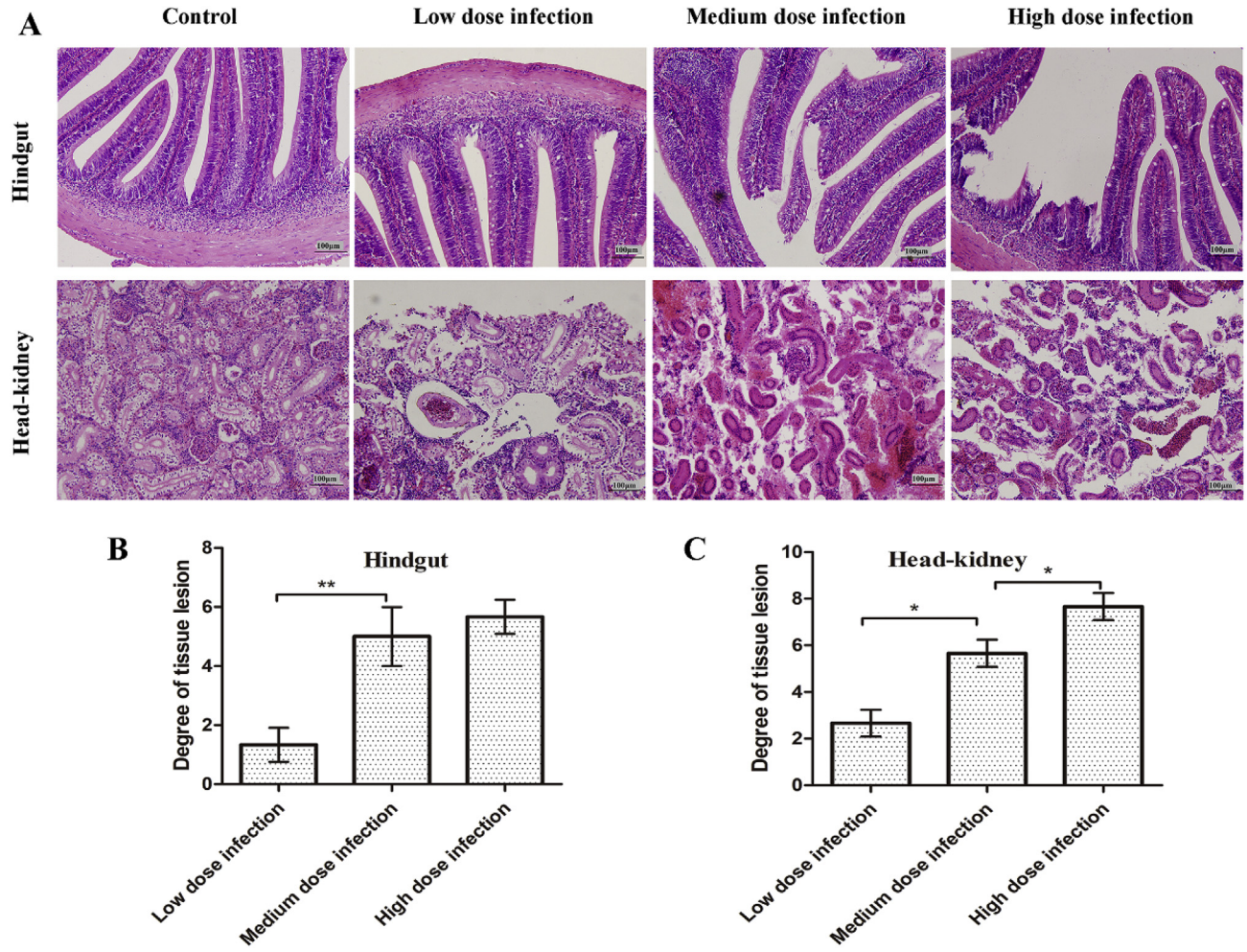

Fig. 5. The relationship between tissue lesions and infection severity. (A) Hematoxylin-eosin staining of the hindgut and head-kidney tissue of crucian carp infected with different concentrations of *A. salmonicida*. (B) Evaluation of tissue lesions in the hindgut after infection with different concentrations of *A. salmonicida*. (C) Evaluation of tissue lesions in the head-kidney after infection with different concentrations of *A. salmonicida*. Statistical analysis (Mann-Whitney test) was conducted using GraphPad Prism software. Error bars indicate standard deviation. **P < 0.01; *P < 0.05.

Q30, and GC content of the clean data were calculated. All the downstream analyses were based on the high-quality clean data. Reference genome and gene model annotation files were downloaded directly from the genome website. HISAT2 was used to build the index of the reference genome and align the paired-end clean reads to the genome.

Differential expression in the two groups was tested, using the DESeq2 R package (1.16.1). The resulting P-values were adjusted using the Benjamini and Hochberg's approach for controlling false discovery rate. Genes with an adjusted P < 0.05 found by DESeq2 were regarded as differentially expressed.

Gene Ontology (GO) enrichment analysis of differentially expressed genes was implemented using the clusterProfiler R package to correct length bias. GO terms with corrected P < 0.05 were considered significantly enriched by differentially expressed genes. We also used clusterProfiler R package to test the statistical enrichment of differentially expressed genes in KEGG pathways.

2.9. Real-time quantitative PCR (RT-qPCR)

The head-kidney and hindgut tissues were collected as described above. After extraction, total RNA was reverse-transcribed into cDNA with a first-strand cDNA synthesis kit (Roche, Basel, Switzerland). The partial sequences of genes were amplified by primers listed in Table 1. β-actin [28] was used as a reference gene. Real-time PCR was carried out with a Mastercycler ep realplex (Eppendorf, Germany) to study the expression of genes in head kidneys. The PCR reaction was performed in a 25 μL volume with a SYBR Premix Ex Taq™ Kit (Takara, Japan), 2 μL of each specific primer and 1 μL of cDNA using the following procedure: initial denaturation at 95 °C for 30 s; followed by 40 cycles of amplification (95 °C for 5 s, 60 °C for 30 s). All assays were performed in triplicate. Relative expression levels were calculated using the $2^{-\Delta\Delta Ct}$ method [29].

2.10. Statistical analyses

qRT-PCR data were reported as mean ± SEM of three independent experiments. Statistical analysis (Student's t-test) was performed using GraphPad Prism 5 (GraphPad Software Inc.).

3. Result

3.1. Isolation and identification of bacteria

The bacteria exhibited a round, smooth surface, with small bulge in the center and neat edge colonies on TSA medium (Fig. 1A), as well as a negative short rod after Gram staining (Fig. 1B). Physiological and biochemical identification results showed that the strain did not grow at 37 °C, did not produce H_2S, neither did it use L-arginine, L-histidine, L-glutamic acid, or L-alanine; it could decompose galactose, arabinose, and mannitol; with the VP test, lysine decarylase were negative but the

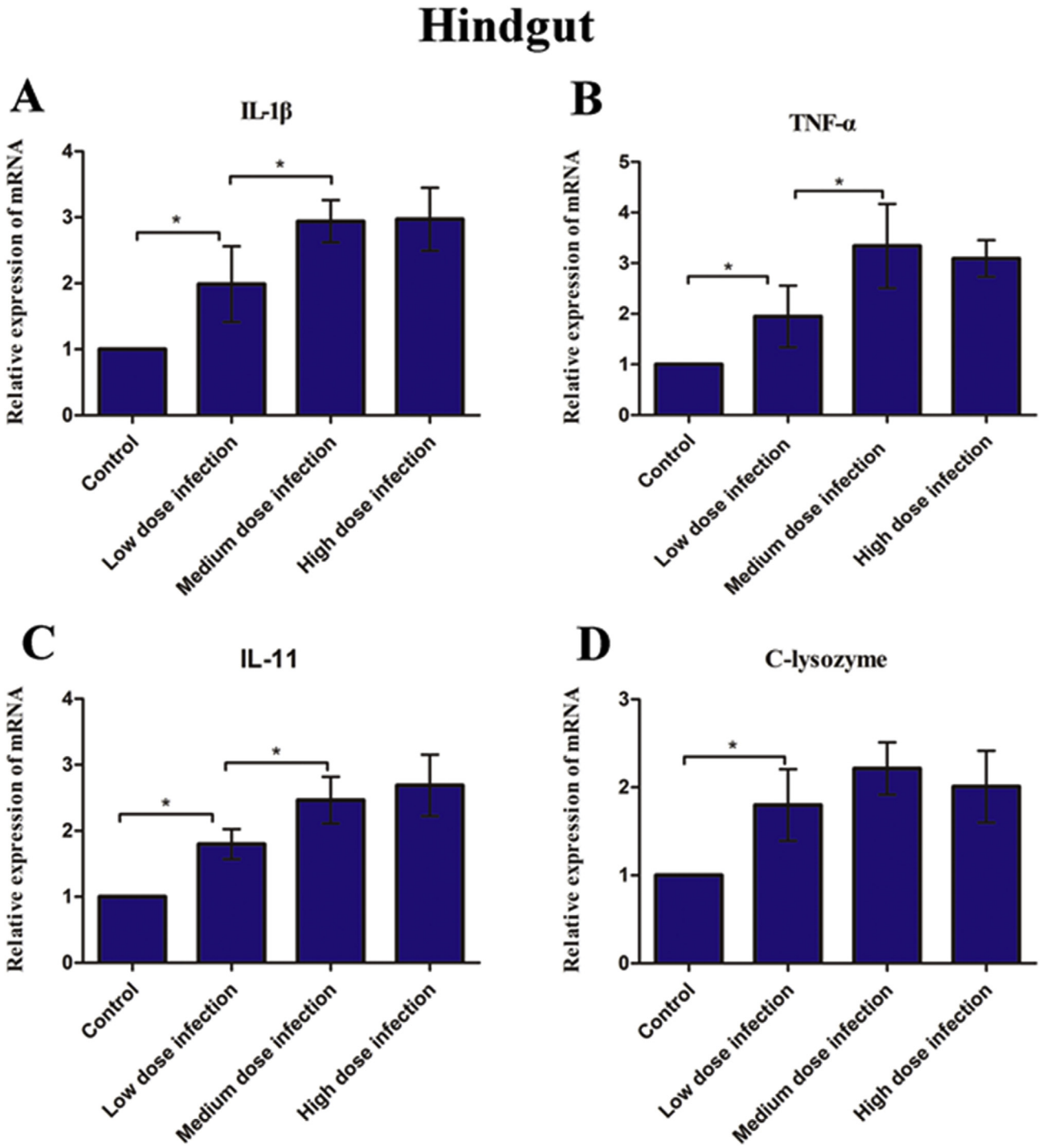

Fig. 6. Relative mRNA expression levels for crucian carp, immune-relevant gene [(A) IL-1β, (B) TNF-α, (C) IL-11 F, (D) C-lysozyme] in hindgut tissue after different concentrations *A. salmonicida* infection. mRNA expression levels are normalized to the reference gene, β-actin. Presented values are the mean values of triplicate sample readings for each fish and tissue. Bars represent mean ± S.E. **P < 0.01; *P < 0.05.

aesculoside, glycerine gas production was positive (Table 2). The nucleic acid fragment of approximately 1500 bp was amplified by PCR, and the sequence size obtained was 1505 bp, which was consistent with the expected result (Fig. 1C). The sequence's similarity to the *A. salmonicida* strain NCIMB 1102 16S ribosomal RNA (NCBI Reference Sequence: NR-118,945.1) was found to be as high as 99% by BLAST alignment in the NCBI database. The phylogenetic tree results showed that the isolated strain (AS110) was closely related to *A. salmonicida* strain (NR-118,945.1) and was on the same clade (Fig. 1D). The above experiment confirmed that the strain was *A. salmonicida* strain NCIMB 1102.

3.2. Diagnosis after regression infection

After the regression infection, the bleeding phenomenon appeared on the surface of the crucian carp in the experimental group. The colony grew in the TSA solid medium coated with the kidney tissue, and its morphological characteristics were similar to those described previously. There were no bleeding symptoms in the control group and no bacterial growth in the medium. The sequencing results of the PCR gel-

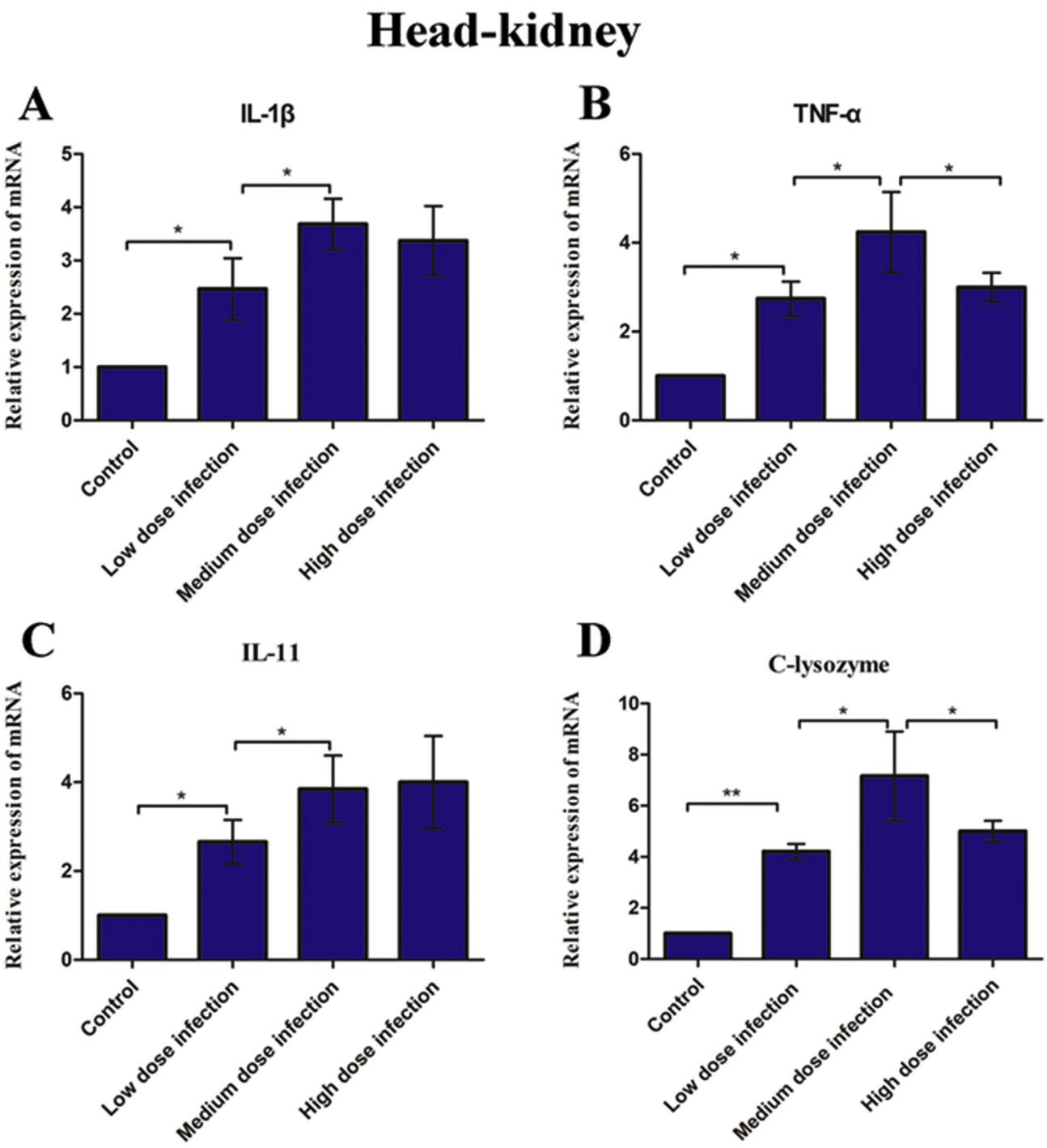

Fig. 7. Relative mRNA expression levels for crucian carp, immune-relevant gene [(A) IL-1β, (B) TNF-α, (C) IL-11 F, (D) C-lysozyme] in head-kidney tissue after different concentrations *A. Salmonicida* infection. mRNA expression levels are normalized to the reference gene, β-actin. Presented values are the mean values of triplicate sample readings for each fish and tissue. Bars represent mean ± S.E. **P < 0.01; *P < 0.05.

recovered products were identical to those of the *A. salmonicida* strain 16S ribosomal RNA gene sequence published by GenBank.

3.3. The mortality rate of crucian carp infected with A. salmonicida

The mortality curve of crucian carp infected with *A. salmonicida* is shown in Fig. 2. Throughout the challenge experiments using different concentrations of the pathogen, we discovered that as the concentration increased, the cumulative mortality also increased. The cumulative mortality (30%) of the crucian carp after low-dose infection was significantly lower than the medium dose (66.6%) and the high dose (90%). However, the mortality rate in the control was 3.3%. In addition, severe bleeding occurred in both dead and living crucian carps, post infection, especially in the mouth and abdomen and around the anus, while no bleeding was observed in the control (Fig. 3).

3.4. Histopathological changes and evaluation of lesion severity induced by A. salmonicida infection

The histopathological examination of the crucian carp showed different degrees of pathological changes, including the proliferation of intestinal mucosal epithelial goblet cells, as some mucosa fell off,

Table 3
Summary of sequencing data quality and the statistics of the transcriptome assemblies.

Sample name	C1[a]	C2[a]	C3[a]	E1[b]	E2[b]	E3[b]
Raw reads	51982674	52763122	53616524	51090740	49683742	51643720
Clean reads	50861076	46370312	45986710	50064430	49643176	46856210
Clean bases	7.63G	6.89G	6.71G	7.51G	7.35G	6.93G
Q20 (%)	98.25	98.61	97.14	94.78	95.32	94.85
Q30 (%)	98.20	98.03	97.86	94.68	94.12	94.85
GC content (%)	46.93	46.57	47.02	47.61	47.58	47.25
Total mapped	88.86%	87.95%	88.03%	89.21%	88.96%	88.53%
Uniquely mapped	82.29%	81.32%	83.16%	82.88%	81.94%	83.28%

[a] C1, C2, C3 indicate libraries derived from the head kidney tissue of control group crucian carp in three biological replicates.
[b] E1, E2, E3 indicate libraries derived from the head kidney tissue of experimental group crucian carp in three biological replicates.

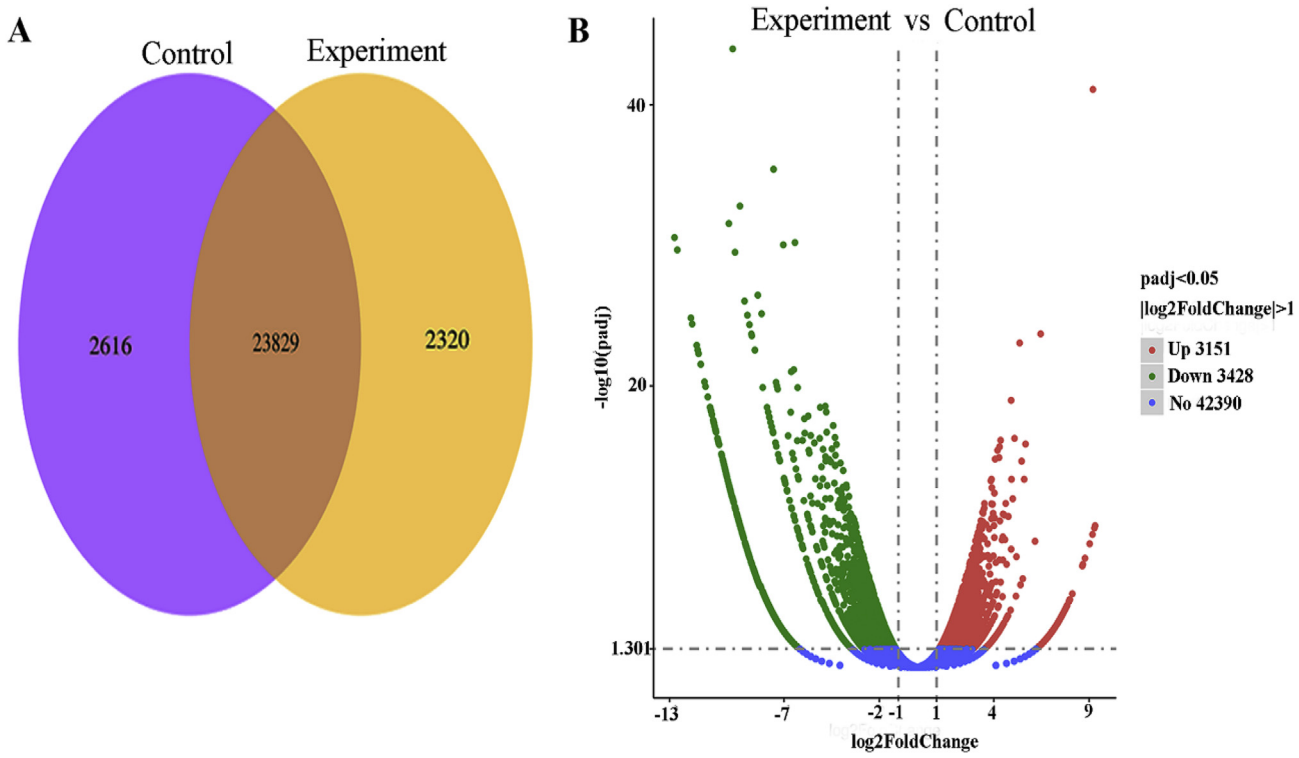

Fig. 8. Comparative results of RNA-seq and differentially expressed gene distributions between the head kidney of control group and experimental group crucian carp. (A) Venn diagram showing genes expressed only in the control group (purple circle), expressed only in the experimental group (yellow circle), and common to both groups (intersection). (B) Volcano plot of DEGs. The X-axis indicates the fold change of expression level of DEGs, and the Y-axis presents significance of differential expression. The blue pots mean no significantly change genes, while the red pots and the green pots indicate up-regulated and down-regulated genes, respectively. (For interpretation of the references to color in this figure legend, the reader is referred to the Web version of this article.)

Table 4
Four C-type lysozyme genes found in all DEGs.

Gene name	Gene length	log2 fold change[a]	P-value[b]	Padj[c]
LOC113042456	946	9.1977	3.29E-46	8.04E-42
LOC113073083	977	6.4548	7.27E-28	1.98E-24
LOC113073087	671	8.7808	1.70E-10	1.79E-08
LOC113066219	683	2.3091	7.99E-08	4.36E-06

[a] The ratio of gene expression levels between the experimental group and the control group was processed by the differential analysis software contraction model, and finally a base-2 logarithmic.
[b] The value of the significance test.
[c] P value after multiple hypothesis test correction.

infiltration by lymphocytes (Fig. 4B); disorderly arrangement, degeneration and necrosis of the liver cells (Fig. 4D); spleen hemorrhage, inflammatory cell infiltration (Fig. 4F); turbidity, swelling, degeneration and necrosis of the renal tubular epithelial cells, with unclear cell boundaries (Fig. 4H).

Following the infection of the crucian carp with different concentrations of bacteria, it was found that the severity of the lesion increased with the increase in pathogen concentrations. The difference in the severity of the lesions between the low-dose infection and the mid-dose infection in the hindgut was extremely significant ($P < 0.01$); there was significant difference ($P < 0.05$) between each group in the head kidney tissues (Fig. 5).

3.5. The relationship between the severity of infection and immune response

After infection with the bacteria at different concentrations, we performed qRT-PCR analysis of four important immune-related genes (TNF-α, IL-1β, IL-11, C-lysozyme) in the hindgut and head-kidney tissues of crucian carp. The results showed that the relative expression levels of four immune-related genes in the hindgut and head-kidney were significantly up-regulated, compared with the control group after infection at different concentrations ($P < 0.05$). The medium-dose was

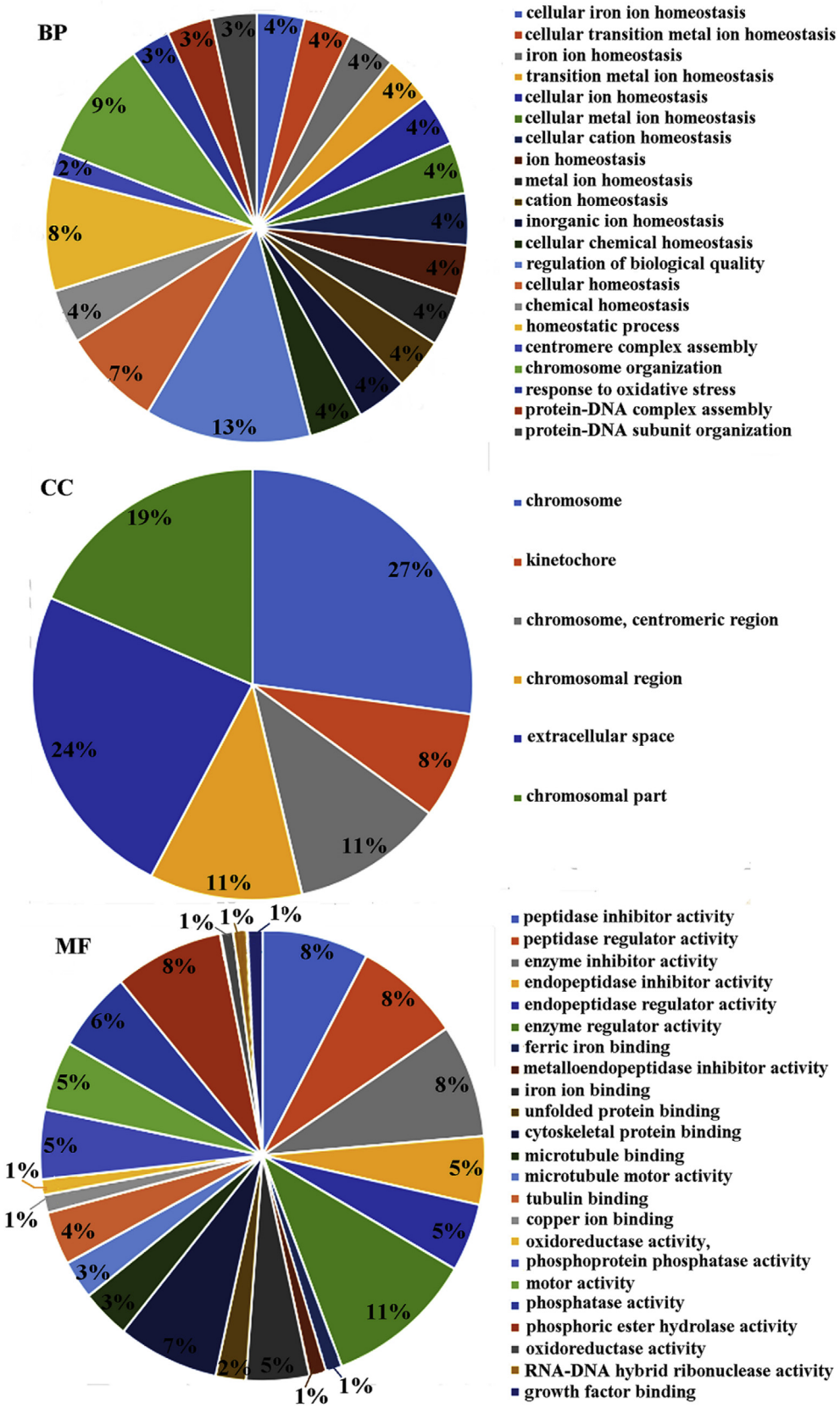

Fig. 9. Gene Ontology (GO) analysis of differentially expressed genes after *A. salmonicida* infection. Genes were annotated by biological process, cellular component, and molecular function.

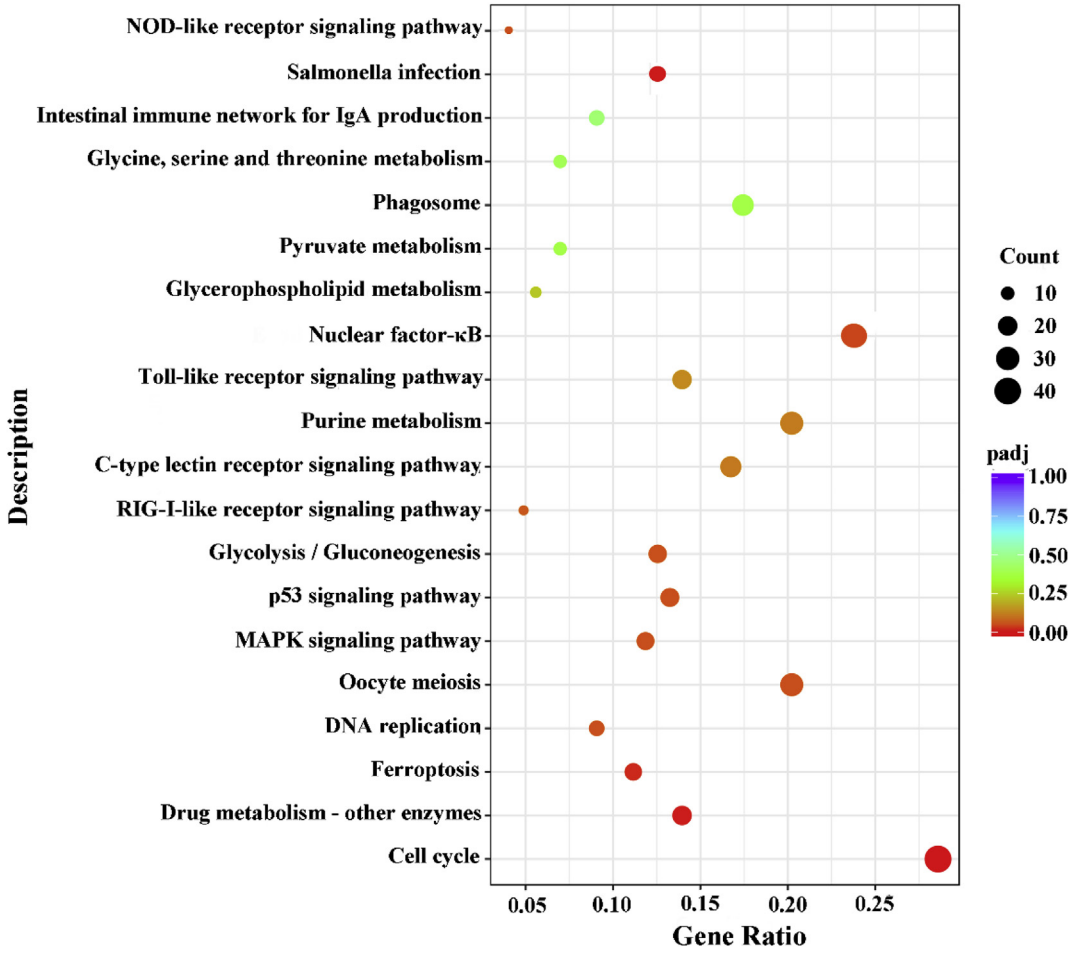

Fig. 10. Scatterplot of KEGG pathways enriched in the differentially expressed genes (DEGs), the abscissa is the ratio of the number of differential genes on the KEGG pathway to the total number of differential genes, the ordinate is the KEGG pathway, the size of the dots represents the number of genes annotated to the KEGG pathway, and the color from red to purple represents significant enrichment. (For interpretation of the references to color in this figure legend, the reader is referred to the Web version of this article.)

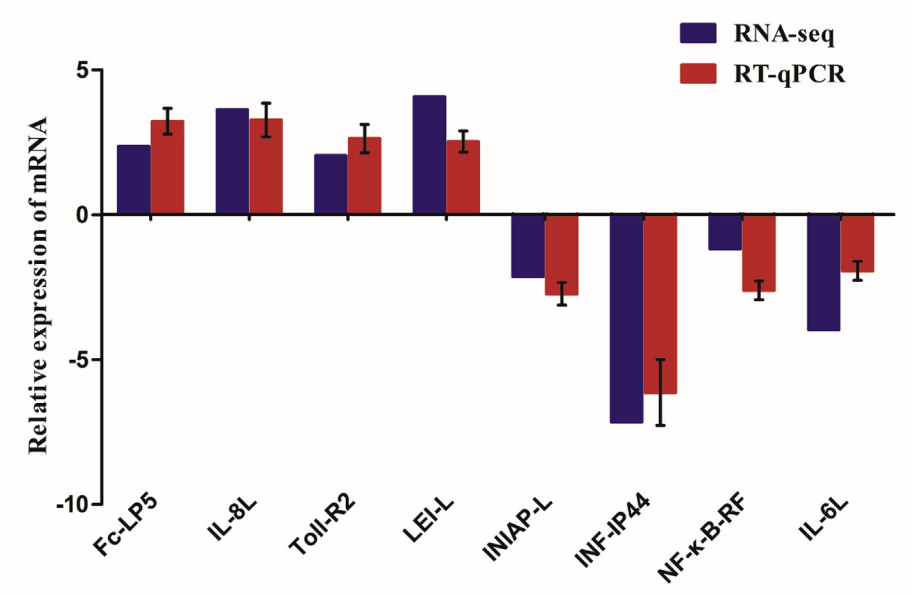

Fig. 11. Comparison of differential gene expression levels by RNA-seq and RT-qPCR methods. Statistical analysis (Student's t-test) was conducted using GraphPad Prism software. Error bars indicate standard deviation.

also significantly up-regulated ($P < 0.05$) compared with the low-dose infection. In hindgut, however, there was no significant difference between high-dose and medium-dose infections. Moreover, TNF-α and C-lysozyme were down-regulated ($P < 0.05$) in the high-dose infection compared with the medium dose in the head-kidney (Fig. 6, Fig. 7).

3.6. Preliminary statistical analysis of RNA-seq data

Six cDNA libraries, consisting of three each from the control (C1, C2, C3) and infection (E1, E2, E3) groups were constructed and analyzed by high-throughput sequencing. An overview of the readings and mass filtration of the six libraries is given in Table 3. A total of 310,780,522 raw readings were obtained. After trimming and filtering the original readings, 289, 781, 914 clean readings were generated from the six libraries. In addition, Clean bases, Q20, Q30, and GC content (%), Total mapped, uniquely mapped for each library, are listed in Table 2. All libraries had a Q20 ratio ≥94.78% and Q30 ratio ≥94.12%.

3.7. Identification and analysis of differentially expressed genes

A total of 28,765 genes were obtained from both groups and mapped into the crucian carp genome. In both groups, 23,829 genes were expressed, of which 2616 and 2320 were from the control and experimental groups respectively (Fig. 8A). By pairing and comparing data, 6579 DEGs with p-value < 0.05 were identified between the control and experimental groups. Among them, 3428 genes were down-regulated, and 3151 genes were up-regulated (Fig. 8B). In addition, Four C-type lysozyme genes found in all DEGs were significantly up-regulated after infection (Table 4).

3.8. GO and KEGG enrichment analysis of the DEGs

In order to further analyze the function of differentially expressed genes, all DEGs were enriched by Blast2 (padj < 0.05). To compare the experimental and control groups, the DEGs were classified into three (Fig. 9): biological processes, cellular components and molecular functions. In the biological processes, the DEGs were mainly enriched in the regulation of biological quality, chromosome organization, iron ion homeostasis, homeostatic process, response to oxidative stress, etc.; in the cellular components, it was concentrated in the chromosome and cellular components; for the molecular function, it was mainly enriched in the enzyme regulator activities, enzyme inhibitor activities, iron ion binding, cytoskeletal protein binding, etc. KEGG pathway enrichment analysis revealed that DEGs were mainly enriched in the cell cycle, drug metabolism, ferroptosis, DNA replication, including some inflammation and immune-related MAPK, NF-κB, TLR, and NLR signaling pathways (Fig. 10).

3.9. Validation of RNA-seq data by RT-qPCR

RT-qPCR was used to validate the reliability of RNA-seq results. We selected 8 immune-related genes from RNA-seq data to verify their mRNA expression levels, including 4 up-regulated genes: Fc receptor-like protein 5 (Fc-LP5), interleukin-8-like (IL-8L), toll-like receptor 2 type-2 (Toll-R2), and leukocyte elastase inhibitor-like (LEI-L); and four down-regulated genes, which are innate immunity activator protein-like (INIAP-L), interferon-induced protein 44-like (INF-IP44), NF-kappa-B-repressing factor-like (NF-κ-B-RF), and Interleukin-6-like (IL-6L). The results show that the data from the RT-qPCR analysis are similar to the RNA-seq data (Fig. 11).

4. Discussion

Atypical furunculosis is an important problem in the farming of salmonids and various other fish species caused by a heterogeneous group of atypical *A. salmonicida* strains. The increased diversity of fish species in aquaculture provides better opportunity for disease interaction between the established species [30]. Crucian carp, is a widely cultivated freshwater fish in china, which is often infected by *A. salmonicida* [7,8]. However, the regulation of its genes and tissue lesions after infection are still unclear. As far as we know, this is the first report of crucian carp infection by *A. salmonicida* through transcriptome and histopathology.

Cell structure changes and cell dysfunction are the basis of all diseases. Histopathological studies can directly and accurately reflect the pathological changes of tissues and cells, providing a reliable basis for future clinical treatment and disease diagnosis. Our histopathological examination found that the crucian carp infected with *A. salmonicida* mainly showed severe bleeding on the surface, especially in the oral cavity and ventral side and around the anus. The internal organs also showed different degrees of pathological changes. The intestinal barrier serves as an important defense, which can effectively prevent bacteria and endotoxins from transferring into the body [31]. Once the barrier is breached, bacterial antigens and microbial products from the intestine can cross the barrier into the liver, kidneys, and other tissues through the portal vein, followed by systemic symptoms [32,33]. In our study, infected crucian carp intestinal epithelial goblet cells showed obvious hyperplasia (part of the mucosa fell off) and lymphocytes infiltration (Fig. 4). In the intestinal mucosal barrier, mucus secreted by goblet cells forms a barrier on the surface of the intestinal mucosal epithelium [34], which plays an important role in resisting invasion by foreign bacteria and intestinal microbes and regulating microbial and host immune responses [35]. Moreover, it is the material basis for mucosal immune effector attachment and exerting immune clearance [36]. Therefore, damage to the intestinal mucosal barrier of the crucian carp after infection may be one of the causes of liver, spleen and kidney and systemic symptoms. Moreover, this also proves that the goblet cells in the intestine of the fish have an important role in resisting the infection of *A. salmonicida*.

Transcriptome analysis helps to understand changes in host cell genes during host-pathogen interactions. In particular, it can reflect the strategy of the host's immune system after activation by the pathogen and how the pathogen overcomes the host-mediated immune response. We found that there were 6,579 DEGs in the infected crucian carp head kidney, of which 3,428 were down-regulated and 3,151 were up-regulated. They were mainly clustered in biological functions such as enzyme regulation activity, response to oxidative stress, and iron ion homeostasis. In cells, many enzymes, such as peroxidase, catalase and superoxide reductase, help protect against oxidative stress [37,38]. Various regulatory factors affecting the expression level of gene transcription are involved in the response of bacteria to oxidative stress [39]. When the host is infected with pathogens, the immune system can produce reactive oxygen species (ROS) to protect against infection [40]. However, ROS is a kind of oxidative stress that is toxic to the cell, and they can cause damage to proteins, DNA and lipoid [41,42], therefore, the cell has to harbor the oxidative stress response for its survival. In addition, iron is an essential component of hemoglobin, myoglobin, and other respiratory enzymes (cytochrome oxidase, catalase, peroxidase). Its main function is to transport oxygen to tissue cells and transport electrons during cell oxidation. Therefore, after crucian carp is infected by *A. salmonicida*, the regulation of these three biological functions plays an important role in maintaining the homeostasis of the body environment and resisting pathogen infection.

More importantly, these DEGs are also clustered into signaling pathways related to inflammation and immunity, such as MAPK, NF-κB, TLR, and NOD-like signaling pathways. The study found that when the pathogen infects the host, it uses pattern recognition receptors (PRR) to non-specifically identify various pathogenic substances [43]. There are two main types of PRR, one is the TLR located on the surface of the cell membrane or on the intima, another is NLR located in the cytoplasm. Host cells can recognize pathogen-associated molecular patterns

(PAMPs) using different PRRs, then activate MAPK and NF-κB signaling pathway, thereby initiating transcription of downstream anti-infective related genes and inflammatory factors and antagonizing the infection of pathogenic bacteria [43–45]. In addition, TLR2 and TLR4 in the TLR family can also mediate rapid activation of MAPK and ROS production [46,47]. In fact, when PAMP is recognized by different PRRs, it can synergistically induce an inflammatory response and indicate a complex adaptive immune response. During the interaction between pathogens and host cells, most effector proteins of pathogens can interfere with host inflammatory response through these two pathways. Therefore, these three immune-related pathways in crucian carp are as important as they are in mammals for resisting the immune response of pathogens.

In fish, the innate immune response is the first line of defense against invading pathogens [48]. Lysozymes (C-type and G-type), are among the important non-specific immune factors for fish defense against pathogenic microorganisms [49,50]. In this study, after the crucian carp was infected, the four C-lysozyme genes found in all DEGs were significantly up-regulated, up to 9.19 fold (Table 4). In previous studies, C-lysozyme transcription product was found to be highest in crucian carp kidneys and lowest in the gill [51]. Moreover, after *Paralichthys olivaceus* was infected with *Edwardsiella ictaluri*, the expression of C-lysozyme in the head-kidney was significantly increased. In addition, after grouper was stimulated by lipopolysaccharides, *Vibrio alginolyticus* and *Singapore grouper iridovirus*, the expression of C-lysozyme in the head and kidney tissues also increased to different degrees [52]. These conclusions are the same as our findings. Therefore, the C-lysozyme of crucian carp plays an important role in the infection against *A. salmonicida*. Moreover, in the future, recombinant C-lysozyme can be applied to feed additives to reduce drug residues and solve bacterial tolerance problems.

In conclusion, through transcriptomics, we have shown the main biological functions and immune-related signaling pathways of DEGs clustering in crucian carp, with atypical *A. salmonicida* infection. We have also shown the relationship between the severity of the infection and histological changes and immune responses, thereby laying a foundation for further research on the immune mechanism and tissue lesion characteristics of crucian carp against *A. salmonicida,* and providing a theoretical basis for future diagnosis and prevention of *A. salmonicida* infection.

Funding

The current study was supported by a grant from the Lanzhou Talent Innovation and Entrepreneurship Project (2017-RC-72) and the Gansu Flying Scholar Special Appointment Project.

Conflicts of interest

The authors declare no conflict of interest.

References

[1] S. Menanteauledouble, G. Kumar, M. Saleh, et al., Aeromonas salmonicida: updates on an old acquaintance, Dis. Aquat. Org. 120 (1) (2016) 49–68.
[2] T. Wiklund, I. Dalsgaard, Occurrence and significance of atypical Aeromonas salmonicida in non-salmonid and salmonid fish species: a review, Dis. Aquat. Org. 32 (1) (1998) 49–69.
[3] A.T. Vincent, A. Fernández-Bravo, M. Sanchis, et al., Investigation of the virulence and genomics of Aeromonas salmonicida strains isolated from human patients, Infect. Genet. Evol. 68 (2019).
[4] R. Tewari, M. Dudeja, S. Nandy, et al., Isolation of aeromonas salmonicida from human blood sample: a case report, J. Clin. Diagn. Res. 8 (2) (2014) 139–140.
[5] C. Dias, M. Ribeiro, A. Correia-Branco, et al., Virulence, attachment and invasion of Caco-2 cells by multidrug-resistant bacteria isolated from wild animals, Microb. Pathog. (128) (2019) 230–235.
[6] M.C. Fontes, M.J. Saavedra, C. Martins, et al., Phylogenetic identification of Aeromonas from pigs slaughtered for consumption in slaughterhouses at the North of Portugal, Int. J. Food Microbiol. 146 (2) (2011) 118–122.
[7] J.E. Han, J.H. Kim, S.P. Shin, et al., Draft genome sequence of aeromonas salmonicida subsp. achromogenes AS03, an atypical strain isolated from crucian carp (Carassius carassius) in the Republic of Korea, Genome Announc. 1 (5) (2013) 1–13.
[8] S. Wistbacka, Lars-Gustaf Lönnström, E. Bonsdorff, et al., Thiaminase activity of crucian carp Carassius carassius injected with a bacterial fish pathogen, aeromonas salmonicida subsp. salmonicida, J. Aquat. Anim. Health 21 (4) (2009) 217–228.
[9] R.C. Cipriano, B. Austin, P.T.K. Woo, et al., Furunculosis and Other Aero Monad Diseases [M] vol. 3, CABI, Wallingford, 2011, pp. 424–483.
[10] I.R. Bricknell, T.J. Bowden, D.W. Bruno, et al., Susceptibility of Atlantic halibut, Hippoglossus hippoglossus to infection with typical and atypical Aeromonas salmonicida, Aquaculture 175 (1–2) (1999) 0–13.
[11] H. Hellberg, E. Moksness, S. Høie, Infection with atypical Aeromonas salmonicida in farmed common wolffish, Anarhichas lupus, J. Fish Dis. 19 (4) (2010) 329–332.
[12] J. Thomas, J. Jerobin, T.S.J. Seelan, et al., Studies on pathogenecity of Aeromonas salmonicida in catfish Clarias batrachus and control measures by neem nanoemulsion, Aquaculture 396–399 (2013) 71–75.
[13] B. Magnadóttir, S.H. Bambir, B.K. Gudmundsdóttir, et al., Atypical Aeromonas salmonicida infection in naturally and experimentally infected cod, Gadus morhua, J. Fish Dis. 25 (2002) 583–597.
[14] O.B. Samuelsen, A.H. Nerland, J. Trond, et al., Viral and bacterial diseases of Atlantic cod Gadus morhua, their prophylaxis and treatment: a review, Dis. Aquat. Org. 71 (3) (2006) 239–254.
[15] H.D. Song, X.J. Sun, M. Deng, et al., Hematopoietic gene expression profile in zebrafish kidney marrow, Proc. Natl. Acad. Sci. 101 (46) (2004) 16240–16245.
[16] F. Liu, D. Wang, J. Fu, et al., Identification of immune-relevant genes by expressed sequence tag analysis of head kidney from grass carp (Ctenopharyngodon idella), Comp. Biochem. Physiol. Genom. Proteonom. 5 (2) (2010) 116–123.
[17] Q. Wan, J. Su, Transcriptome analysis provides insights into the regulatory function of alternative splicing in antiviral immunity in grass carp (Ctenopharyngodon idella), Sci. Rep. 5 (2015) 12946.
[18] M. Norum, J. Bogwald, R.A. Dalmo, Isolation and characterisation of spotted wolffish (Anarhichas minor Olafsen) macrophages, Fish Shellfish Immunol. 18 (5) (2005) 381–391.
[19] K.J. Laing, J.D. Hansen, Fish T cells: recent advances through genomics, Dev. Comp. Immunol. 35 (12) (2011) 1282–1295.
[20] H.W. Ferguson, M.J. Claxton, R.D. Moccia, et al., The quantitative clearance of bacteria from the bloodstream of rainbow trout (Salmo gairdneri), J. Vet. Pathol. 19 (6) (1982) 687–699.
[21] P. Orozova, M. Barker, D.A. Austin, et al., Identification and pathogenicity to rainbow trout,Oncorhynchus mykiss (Walbaum), of some aeromonads, J. Fish Dis. 32 (10) (2010) 865–871.
[22] F. Denoeud, J.M. Aury, C.D. Silva, et al., Annotating genomes with massive-scale RNA sequencing, Genome Biol. 9 (12) (2008).
[23] M.K. Raida, K. Buchmann, Development of adaptive immunity in rainbow trout, Oncorhynchus mykiss (Walbaum) surviving an infection with Yersinia ruckeri, Fish Shellfish Immunol. 25 (5) (2008) 533–541.
[24] F. Sun, E. Peatman, C. Li, et al., Transcriptomic signatures of attachment, NF-κB suppression and IFN stimulation in the catfish gill following columnaris bacterial infection, Dev. Comp. Immunol. 38 (1) (2012).
[25] M.G. George, A.B. Julia, G.L. Timothy, Taxonomic Outline of the Prokaryotes. Bergey's Manual of Systematic Bacteriology, second ed., Springer New York, New York, 2004.
[26] M.A. Hamilton, R.C. Russo, R.V. Thurston, Trimmed Spearman-Karber method for estimating median lethal concentrations in toxicity bioassays, Environ. Sci. Technol. 11 (7) (1977) 714–719.
[27] Y.K. Lia, J.Y. Wu, D. Lia, et al., Transcriptome analysis of spleen reveals the signal transduction of toll-like receptors after *Aeromonas hydrophila* infection in Schizothorax prenanti, Fish Shellfish Immunol. 84 (2019) 816–824.
[28] Y.H. Dong, Y.Y. Yang, J. Liu, et al., Inhibition of *Aeromonas hydrophila*-induced intestinal inflammation and mucosal barrier function damage in crucian carp by oral administration of *Lactococcus lactis*, Fish Shellfish Immunol. 83 (2018) 359–367.
[29] X.D. Ling, W.T. Dong, Y. Zhang, et al., A recombinant adenovirus targeting typical *Aeromonas salmonicida* induces an antibody-mediated adaptive immune response after immunization of rainbow trout, Microb. Pathog. 133 (2019) 103559.
[30] K. Bjarnheidur, B. Björnsdóttir, Vaccination against atypical furunculosis and winter ulcer disease of fish, Vaccine 25 (30) (2007) 0-5523.
[31] K.R. Groschwitz, S.P. Hogan, Intestinal barrier function: molecular regulation and disease pathogenesis, J. Allergy Clin. Immunol. 124 (1) (2009) 3–20.
[32] Fermín Sánchez de Medina, I. Romero-Calvo, et al., Intestinal inflammation and mucosal barrier function, Inflamm. Bowel Dis. 20 (12) (2014) 2394–2404.
[33] H.D. Ma, Y.H. Wang, C. Chang, et al., The intestinal microbiota and microenvironment in liver, Autoimmun. Rev. 14 (3) (2015) 183–191.
[34] Y.S. Kim, S.B. Ho, Intestinal goblet cells and mucins in health and disease: recent insights and progress, Curr. Gastroenterol. Rep. 12 (5) (2010) 319–330.
[35] I.K. Gipson, Goblet cells of the conjunctiva: a review of recent findings, Prog. Retin. Eye Res. 54 (2016) 49–63.
[36] X.F. Wu, M.M. Amorn, P.K. Aujla, et al., Histologic characteristics and mucin immunohistochemistry of cystic fibrosis sinus mucosa, Arch. Otolaryngol. Head Neck Surg. 137 (4) (2011) 383–389.
[37] James A. Imlay, Cellular defenses against superoxide and hydrogen peroxide, Annu. Rev. Biochem. 77 (1) (2008) 755–776.
[38] P.J. Pomposiello, M.H.J. Bennik, B. Demple, Genome-wide transcriptional profiling of the Escherichia coli responses to superoxide stress and sodium salicylate, J. Bacteriol. 183 (13) (2001) 3890–3902.
[39] E.C. Ziegelhoffer, T.J. Donohue, Bacterial responses to photo-oxidative stress, Nat.

Rev. Microbiol. 7 (2009) 1-1.
[40] P. Roch, Defense mechanisms and disease prevention in farmed marine invertebrates, Aquaculture 172 (1–2) (1999) 125–145.
[41] J.A. Imlay, Pathways of oxidative damage, Annu. Rev. Microbiol. 57 (1) (2003) 395–418.
[42] P.R. Ogilby, Singlet oxygen: there is indeed something new under the sun, Chem. Soc. Rev. 39 (8) (2010) 3181–3209.
[43] T. Kawai, S. Akira, The roles of TLRs, RLRs and NLRs in pathogen recognition, Int. Immunol. 21 (4) (2009) 317–337.
[44] Y.M.S. Hsu, Y. Zhang, Y. You, et al., The adaptor protein CARD9 is required for innate immune responses to intracellular pathogens, Nat. Immunol. 8 (2) (2007) 198–205.
[45] M.S. Hayden, S. Ghosh, Signaling to NF-Kb, Genes Dev. 18 (18) (2004) 2195–2224.
[46] C.S. Yang, D.M. Shin, H.M. Lee, et al., ASK1-p38 MAPK-p47phox activation is essential for inflammatory responses during tuberculosis via TLR2-ROS signaling, Cell Microbiol. 10 (3) (2008) 741–754.
[47] A. Matsuzawa, K. Saegusa, T. Noguchi, et al., ROS-dependent activation of the TRAF6-ASK1-p38 pathway is selectively required for TLR4-mediated innate immunity, Nat. Immunol. 6 (6) (2005) 587–592.
[48] Bergljót Magnadóttir, Innate immunity of fish (overview), Fish Shellfish Immunol. 20 (2) (2006) 137–151.
[49] D. Gomez, J.O. Sunyer, I. Salinas, The mucosal immune system of fish: the evolution of tolerating commensals while fighting pathogens, Fish Shellfish Immunol. 35 (6) (2013) 1729–1739.
[50] L. Callewaert, C.W. Michiels, Lysozymes in the animal kingdom, J. Biosci. 35 (1) (2010) 127–160.
[51] M. Wang, X. Zhao, X. Kong, et al., Molecular characterization and expressing analysis of the c-type and g-type lysozymes in Qihe crucian carp Carassius auratus, Fish Shellfish Immunol. 52 (2016) 210–220.
[52] S. Wei, Y. Huang, J. Cai, et al., Molecular cloning and characterization of c-type lysozyme gene in orange-spotted grouper, Epinephelus coioides, Fish Shellfish Immunol. 33 (2) (2012).